

Appendix E FCT Document Cover Sheet

Name/Title of Deliverable/Milestone/Revision No.	Initial Neutronics and Thermal-Hydraulic Coupling for Spent Nuclear Fuel Canister-M3SF-19OR010305015
Work Package Title and Number	Direct Disposal of Dual Purpose Canisters - ORNL, SF-19OR01030501
Work Package WBS Number	1.08.01.03.05
Responsible Work Package Manager	John Scaglione <i>kaushikbanerjee</i>

Date Submitted 09/20/2019

Quality Rigor Level for Deliverable/Milestone	<input checked="" type="checkbox"/> QRL-3	<input type="checkbox"/> QRL-2	<input type="checkbox"/> QRL-1 <input type="checkbox"/> Nuclear Data	<input type="checkbox"/> Lab Participant QA Program (No additional FCT QA requirements)
---	---	--------------------------------	---	---

This deliverable was prepared in accordance with ORNL
(Participant/National Laboratory Name)

QA program which meets the requirements of
 DOE Order 414.1 NQA-1-2000 NQA-1-2008

This Deliverable was subjected to:

Technical Review

Technical Review (TR)

Review Documentation Provided

- Signed TR Report or,
- Signed TR Concurrence Sheet or,
- Signature of TR Reviewer(s) below

Name and Signature of Reviewers

Peer Review

Peer Review (PR)

Review Documentation Provided

- Signed PR Report or,
- Signed PR Concurrence Sheet or,
- Signature of PR Reviewer(s) below

NOTE 1: Appendix E should be filled out and submitted with the deliverable. Or, if the PICS:NE system permits, completely enter all applicable information in the PICS:NE Deliverable Form. The requirement is to ensure that all applicable information is entered either in the PICS:NE system or by using the FCT Document Cover Sheet.

NOTE 2: In some cases there may be a milestone where an item is being fabricated, maintenance is being performed on a facility, or a document is being issued through a formal document control process where it specifically calls out a formal review of the document. In these cases, documentation (e.g., inspection report, maintenance request, work planning package documentation or the documented review of the issued document through the document control process) of the completion of the activity, along with the Document Cover Sheet, is sufficient to demonstrate achieving the milestone. If QRL 1, 2, or 3 is not assigned, then the Lab / Participant QA Program (no additional FCT QA requirements) box must be checked, and the work is understood to be performed and any deliverable developed in conformance with the respective National Laboratory /Participant, DOE or NNSA-approved QA Program.

Reviewers

Requested Release Date Not Provided

Workflow ⓘ

Reviewer

Duration (avg.)

Derivative Classifier <i>Added by keywords</i>	Bill Reich ⓘ	2 days	<input type="text" value="charge number"/>	ⓘ
Technical Editor <i>Required by Reactor & Nuclear Systems Division</i>	Deborah Counce ⓘ	4 days	<input type="text" value="35304D66"/>	ⓘ
Technical Reviewer	Steven Hamilton ⓘ	7 days		ⓘ
Technical Reviewer <i>Required by Reactor & Nuclear Systems Division</i>	Katherine Royston ⓘ	7 days		ⓘ
Supervisor	Thomas Evans ⓘ	3 days		ⓘ
Program Manager <i>Required by Reactor & Nuclear Systems Division</i>	John Scaglione ⓘ	1 days		ⓘ
Export Control <i>Added by keywords</i>	Timothy Busch ⓘ	2 days		ⓘ
Administrative Check <i>Required by Reactor & Nuclear Systems Division</i>	Elaine Davis ⓘ	1 days		ⓘ
Division Approver	Jeremy Busby ⓘ	3 days		ⓘ
Releasing Official	Leesa Laymance ⓘ	3 days		ⓘ

Initial Neutronics and Thermal-Hydraulic Coupling for Spent Nuclear Fuel Canister

Spent Fuel and Waste Disposition

*Prepared for
US Department of Energy
Spent Fuel and Waste Science
and Technology*

*Gregory G. Davidson, Mathew
Swinney, Seth Johnson, Santosh
Bhatt, and Kaushik Banerjee
Oak Ridge National Laboratory*

September 20, 2019
M3SF-19OR010305015
ORNL/SPR-2019/1333

**SFWD Working Document: External Release or
Reference Requires DOE-NE Approval**

This report was prepared as an account of work sponsored by an agency of the United States Government. Neither the United States Government nor any agency thereof, nor any of their employees, makes any warranty, express or implied, or assumes any legal liability or responsibility for the accuracy, completeness, or usefulness of any information, apparatus, product, or process disclosed, or represents that its use would not infringe privately owned rights. Reference herein to any specific commercial product, process, or service by trade name, trademark, manufacturer, or otherwise, does not necessarily constitute or imply its endorsement, recommendation, or favoring by the United States Government or any agency thereof. The views and opinions of authors expressed herein do not necessarily state or reflect those of the United States Government or any agency thereof.

This is a technical report that does not take into account contractual limitations or obligations under the Standard Contract for Disposal of Spent Nuclear Fuel and/or High-Level Radioactive Waste (Standard Contract) (10 CFR Part 961). For example, under the provisions of the Standard Contract, spent nuclear fuel in multi-assembly canisters is not an acceptable waste form, absent a mutually agreed to contract amendment. To the extent discussions or recommendations in this paper conflict with the provisions of the Standard Contract, the Standard Contract governs the obligations of the parties, and this paper in no manner supersedes, overrides, or amends the Standard Contract.

This report reflects technical work which could support future decision making by the Department of Energy (DOE or Department). No inferences should be drawn from this report regarding future actions by DOE, which are limited both by the terms of the Standard Contract and a lack of Congressional appropriations for the Department to fulfill its obligations under the Nuclear Waste Policy Act including licensing and construction of a spent nuclear fuel repository.

ACKNOWLEDGMENTS

This research was sponsored by the Spent Fuel and Waste Science and Technology Program of the US Department of Energy and was carried out at Oak Ridge National Laboratory under contract DE-AC05-00OR22725 with UT-Battelle, LLC.

This page is intentionally left blank.

SUMMARY

This report documents work performed supporting the US Department of Energy (DOE) Nuclear Energy Spent Fuel and Waste Disposition, Spent Fuel and Waste Science and Technology, under work breakdown structure element 1.08.01.03.05, “Direct Disposal of Dual Purpose Canisters.” In particular, this appendix fulfills the M3 milestone, M3SF-19OR010305015, “Multiphysics criticality consequence analysis capability development status report,” as Revision 1 to M3SF-19OR010305016, “Initial neutronic and thermal hydraulic coupling for waste package” within work package SF-19OR01030501, “Direct Disposal of Dual Purpose Canisters–ORNL.”

This report presents the initial development status of a multiphysics criticality consequence simulation framework, Terrenus. Terrenus currently couples two physics codes: the Monte Carlo radiation transport code Shift and the thermal-hydraulics code COBRA-SFS. The coupling capability has been demonstrated using a simplified 3×3 fuel pin lattice. Terrenus will be developed further to include (1) general geometry package support, allowing modeling of a spent nuclear fuel (SNF) cask with all structural details, (2) a depletion solver to determine the change in nuclide composition at the end of each time step, and (3) a mechanics code to determine any structural impact due to a criticality event. Future research and development works include identifying/developing a modern two-phase thermal-hydraulics code and developing an approach to solve fast neutronic transients. The goal of this multiphysics framework is to determine the feasibility of direct disposal of currently loaded SNF canisters by including or excluding a criticality event from a repository performance analysis framework in terms of consequences.

The revision 1 to this report includes extending Terrenus to a 17×17 pressurized water reactor (PWR) fuel assembly. We also investigated the phenomena necessary to quench a critical reaction, and investigated the water level necessary to achieve criticality in a typical canister. Finally, we describe the initial implementation of a critical power search capability.

This page is intentionally left blank.

CONTENTS

ACKNOWLEDGMENTS	iii
SUMMARY	v
LIST OF FIGURES	ix
LIST OF TABLES	xi
REVISION HISTORY.....	xiii
ACRONYMS	xiv
1. INTRODUCTION	1
1.1 Scope	2
2. METHODOLOGY	3
2.1 Concept	3
2.2 Numerical codes.....	6
2.2.1 Shift.....	6
2.2.2 COBRA-SFS.....	7
2.3 Assumptions.....	7
2.4 Initial Configuration and Input Data	7
3. RESULTS AND DISCUSSION.....	11
3.1 Power Distribution	11
3.2 Channel Temperatures Distributions.....	13
3.3 Channel Density Distributions	15
4. CONCLUSION	17
5. REFERENCES	19
Appendix A	A-1
A.1 Use of Terrenus on 17×17 PWR Assembly	A-1
A.2 Investigation of Negative Reactivity Phenomena	A-4
A.3 Calculating Critical Water Level	A-6
A.4 Initial Implementation of Critical Power Search	A-8
A.5 Conclusions and Future Work.....	A-8

This page is intentionally left blank.

LIST OF FIGURES

Figure 1. Flowchart Showing Inner Radiation Transport Thermal-Hydraulic Coupling Loop, Outer Mechanics, and Nuclide Depletion Loop.	3
Figure 2. Multiphysics Coupling for a DPC Simulator for Solving Steady-State or Gradual Approach to Critical Configuration Problems.	5
Figure 3. Schematic of 3×3 Square Array of Spent Fuel Rods within a Canister. (The left image shows the COBRA-SFS channel, rod, and slab nodalization.).....	10
Figure 4. 3×3 Radial Power Distribution over 10 Iterations at $z = 185$ cm.	12
Figure 5. 4×4 Channel Temperatures over 10 Iterations at $z = 185$ cm.....	14
Figure 6. Axial Temperatures Distributions for Iterations 0 and 1.....	15
Figure 7. Channel Water Densities.	15
Figure 8. Axial Channel Water Densities in a Central Channel.	15
Figure A.1. Pin Layout of a Standard 17×17 PWR Assembly	A-1
Figure A.2. Relative Pin Powers at the Axial Midplane (<i>Left</i>) and Axial Distribution of Relative Pin Power along a Fuel Pin adjacent to the Central Instrument Tube (<i>right</i>).....	A-2
Figure A.3. Temperature of the Water Moderator in Each Channel at the Axial Midplane (<i>left</i>) and Axial Temperature Distribution in the Central Instrument Tube (<i>right</i>).	A-2
Figure A.4. Water Moderator Density in Each Channel at the Axial Midplane (<i>left</i>) and Axial Distribution of the Moderator Density in the Central Instrument Tube (<i>right</i>).....	A-3
Figure A.5. Pin Temperature in Each Pincell at the Axial Midplane (<i>left</i>) and the Axial Temperature Distribution in a Fuel Pin adjacent to the Central Instrument Tube (<i>right</i>).	A-3
Figure A.6. Axial Distribution of Temperature (<i>left</i>) and Moderator Density (<i>right</i>) in the Central Instrument Tube for Various Power Levels.....	A-4
Figure A.7. Reactivity in a Fully Reflected 17×17 PWR Assembly at Various Power Levels.	A-4
Figure A.8. A Simplified Neutronic Model of a Loaded Canister.....	A-5
Figure A.9. Effect of Moderator Density on Reactivity.	A-6

This page is intentionally left blank.

LIST OF TABLES

Table 1. Description of the Fuel Rod.....	9
Table 2. Fuel Rod's Material Properties	9
Table 3. Description of the Square Box and Canister.....	9
Table 4. Fluid Properties	9
Table A.1. Critical Water Level for the MPC-32-TSC 079 Sequoyah Canister.....	A-6
Table A.2. Test Cases for Critical Water Level Search.....	A-7

This page is intentionally left blank.

REVISION HISTORY

Revision	Changes Made
0	Initial issue
1	Appendix A is added in this revision, which details the modeling of a 17x17 PWR assembly, investigation of reactivity quenching phenomena, and an investigation of the water level necessary to induce criticality.

ACRONYMS

ASCR	Advanced Scientific Computing Research Project
BWR	boiling water reactor
CAD	computer-aided design
CASL	Consortium for Advanced Simulation of Light Water Reactors
CFD	computational fluid dynamics
DOE	US Department of Energy
DPC	dual-purpose canister
ECP	Exascale Computing Project
FEPs	features, events, and processes
GG	general geometry
GPU	graphics processing unit
I/O	input/output
MCNP	Monte Carlo N-Particle
MPI	message passing interface
NE	Office of Nuclear Energy
ORNL	Oak Ridge National Laboratory
PA	performance assessment
PWR	pressurized water reactor
RTK	reactor toolkit
SFS	[COBRA] Spent Fuel Storage
SFWD	Spent Fuel and Waste Disposition
SNF	spent nuclear fuel

This page is intentionally left blank.

SPENT FUEL AND WASTE DISPOSITION PROGRAM INITIAL NEUTRONICS AND THERMAL-HYDRAULICS COUPLING FOR SPENT NUCLEAR FUEL CANISTER

1. INTRODUCTION

This report documents work performed supporting the US Department of Energy (DOE) Nuclear Energy Spent Fuel and Waste Disposition, Spent Fuel and Waste Science and Technology, under work breakdown structure element 1.08.01.03.05, “Direct Disposal of Dual Purpose Canisters.” In particular, this appendix fulfills the M3 milestone, M3SF-19OR010305015, “Multiphysics criticality consequence analysis capability development status report,” as Revision 1 to M3SF-19OR010305016, “Initial neutronic and thermal hydraulic coupling for waste package” within work package SF-19OR01030501, “Direct Disposal of Dual Purpose Canisters–ORNL.”

Dual-purpose (storage and transportation) canisters (DPCs) are presently used to store spent nuclear fuel (SNF) at reactor sites. DPCs are not designed, licensed, or loaded with considerations of geological disposal conditions and requirements. Already, ~3,000 SNF dry storage systems have been loaded in the United States, and the majority of dry storage systems loaded are DPCs [1]. US utilities are loading approximately 300 DPCs annually. Therefore, the United States has a large number of loaded DPCs, and the DPC inventory is expected to increase at a steady pace in the coming years. Direct disposal of DPCs has the potential to avoid or reduce the amount of repackaging of commercial SNF, which can have significant financial and dose liabilities. Moreover, DPCs would be required to be disposed of as a low-level waste in the absence of direct disposal of DPCs. The DOE Office of Nuclear Energy (NE) is currently investigating the feasibility of direct disposal of DPCs in a geological repository to potentially offset the need to repackage the currently loaded SNF into smaller disposable canisters. Although it has been indicated [2] that direct disposal of DPCs is feasible from a purely technical perspective, several engineering challenges, along with legal and policy issues, must be addressed to make DPC disposal a reality. One challenge is the potential for post-closure criticality in a repository time frame.

A repository performance assessment (PA) includes investigation of a sequence of features, events, and processes (FEPs) that might affect the repository performance. Criticality is considered an event within the FEPs that has the potential to affect overall repository performance. The FEPs that can affect repository performance are screened for inclusion or exclusion in a PA. An FEP can be excluded based on a low-probability criterion, a low-consequence criterion, and/or by regulation. It has been demonstrated that many loaded DPCs have the potential to achieve critical configurations under specific conditions over a repository time frame of 10,000 years or longer [3]. This is mainly due to the aluminum-based neutron absorbers used in the DPCs that are not expected to provide criticality control, especially in an aqueous environment and over repository performance periods of thousands of years. Therefore, reliance on the low probability criterion for excluding criticality event from a repository PA may not be a feasible option for DPC direct disposal, unless preconditioning DPCs with filler materials to prevent DPC flooding over a repository performance period emerges as a viable alternative. The other option to support DPC direct disposal is to perform a criticality consequence analysis to determine the impact of a potential criticality event on a repository PA for either exclusion (low consequence) or inclusion of criticality.

The potential consequences include an increase in radionuclide inventory, ambient temperature, and associated system (DPC) pressure. The consequences associated with criticality events internal to DPCs have not been specifically analyzed, and a fully coupled analysis capability allowing simulation of various postulated criticality sequences to evaluate associated consequences does not currently exist. This report presents the initial development status of a new multiphysics framework, Terrenus. Terrenus will

initially provide a high-fidelity quasistatic criticality event simulation capability by coupling associated physics such as neutronics, thermal-hydraulics, and mechanics. The Terrenus framework may be further extended to support a transient criticality event with a time-dependent neutronics solver. In this context, it is important to note that the criticality consequence analysis approach has been discussed in detail in the Yucca Mountain *Disposal Criticality Analysis Methodology Topical Report* [4].

Section 2 of this report presents the methodology. Results and discussions are provided in Section 3, and Section 4 provides the conclusion.

1.1 Scope

This report presents the initial development of neutronics and thermal-hydraulics coupling for simulating criticality related physics. This report also applies only to DPCs containing commercial pressurized water reactor (PWR) or boiling water reactor (BWR) SNF. Only in-canister configurations are considered; external configurations that may lead to a criticality event—external criticality—are not part of the scope of the current investigation.

2. METHODOLOGY

Simulating SNF within a DPC in a geological repository requires high-fidelity multiphysics simulations. The relevant physics include (1) radiation transport for calculating the system reactivity and the distribution of fission power throughout the fuel in a canister, (2) thermohydraulics for calculating the density and temperature of any water within the canister, as well as the fuel temperature, (3) nuclide depletion for calculating the changing nuclide inventory over time, and (4) mechanics for calculating the stress and strain on the canister walls and inner structure. This coupling is described in more detail in Section 2.1. This report demonstrates an initial coupling capability between a high-performance Monte Carlo radiation transport solver (Shift) and a subchannel single-phase thermal-hydraulics code featuring natural circulation (COBRA- Spent Fuel Storage [SFS], also referred to as COBRA in this document).

2.1 Concept

As described above, the relevant physics necessary for a DPC simulator include radiation transport, thermal-hydraulics, depletion, and mechanics. For a steady-state or gradual approach to a critical configuration, the coupling between the physics packages is given in Figure 1. A rapid approach to criticality involves different physics (radiation transport and kinetics). While simulation capabilities for these types of problems are being investigated, they are outside the scope of this report.

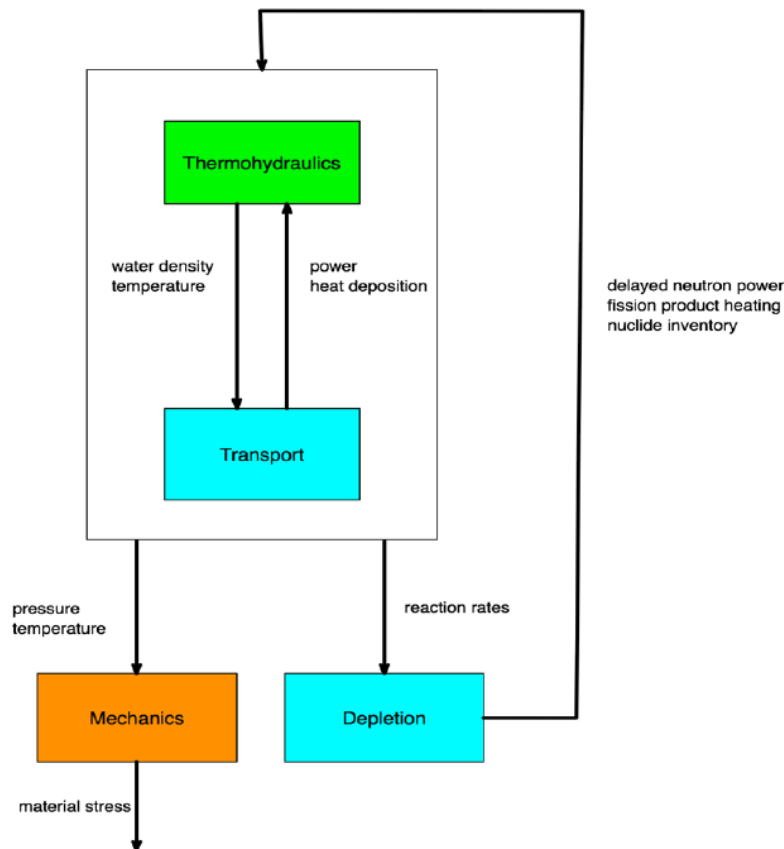


Figure 1. Flowchart Showing Inner Radiation Transport Thermal-Hydraulic Coupling Loop, Outer Mechanics, and Nuclide Depletion Loop.

The coupling for a gradual approach to criticality in a DPC simulator is in two loops. The first inner loop couples the quasi-static radiation transport equations to a thermal-hydraulics solver. These two physics

packages are iterated to convergence for a particular point in time. The second outer loop involves (1) the mechanics solver, which uses the converged fluid properties to calculate stress and strain on the DPC's wall and internal structures, and (2) the depletion solver, which uses the converged fission power to deplete the nuclide inventory and advance the simulation to the next time point.

The scope of this milestone includes the initial coupling of the quasi-static high-fidelity radiation transport code Shift to the subchannel natural circulation code COBRA-SFS. Coupling COBRA-SFS to Shift requires overcoming several technical hurdles. The primary difficulty is designing an efficient interface between a serial input-output (I/O)-based process (COBRA) and a massively parallel framework (Shift). The parallel program has a comparatively large startup cost, so it is desirable to provide Shift an in-memory interface that allows the code to remain active but idling while COBRA generates updated thermal hydraulics data. A Python-based driver code that launches and coordinates the Shift and COBRA processes achieves this design goal.

The Python driver code has three main responsibilities: interaction with COBRA, interaction with Shift, and coordination between the two. Since COBRA uses an inflexible input format and a human-readable output format, the driver must be able to generate text-based fixed column input from numerical data. The input format for COBRA has several limitations that affect the accuracy of the simulation. The most serious of these is that COBRA's input allows only an axial power profile and a separate radial power profile, implying that the 3D power distribution calculated by Shift must be approximated by a separable function in r and z . An additional limitation is in the fixed-column input format: most variables must be represented in fixed-point notation inside five or ten columns, limiting both the accuracy and the range of values that can be provided to COBRA. Finally, since COBRA uses the imperial system of units, care must be taken to properly convert values to and from Shift. To ensure the validity of the conversions, the Python driver parses the units of each field in the output and uses an open source unit conversion package to maintain the integrity of the units throughout the code.

Shift's thermal hydraulics API uses a parallel HDF5-format interface to efficiently read, distribute, and write its thermal-hydraulics and neutronics data. Since it has this computer-readable, metadata-rich I/O interface, robustly providing input to and reading output from Shift is very simple. The major challenge of coupling to Shift is informing the code when new input is available and determining when newly generated output can be safely read. This is addressed by using special command tokens piped through stdin and stdout between the Shift message passing interface (MPI) executable and the Python driver code.

The final task for the Python driver is to asynchronously run and coordinate the COBRA and Shift processes. Figure 2 represents the driver as a flow chart. The two gray regions are internal components that manage execution of COBRA and Shift. They run independently using Python's `asyncio` module, which allows the driver process to interleave input, output, and command execution between the two codes. This allows processing of the COBRA output file to complete while Shift is still solving the neutronics. In the flow chart, the dashed blue arrows represent the flow of data between the two processes. When Shift reports convergence, or if either code fails unexpectedly, then the driver cleanly terminates both codes.

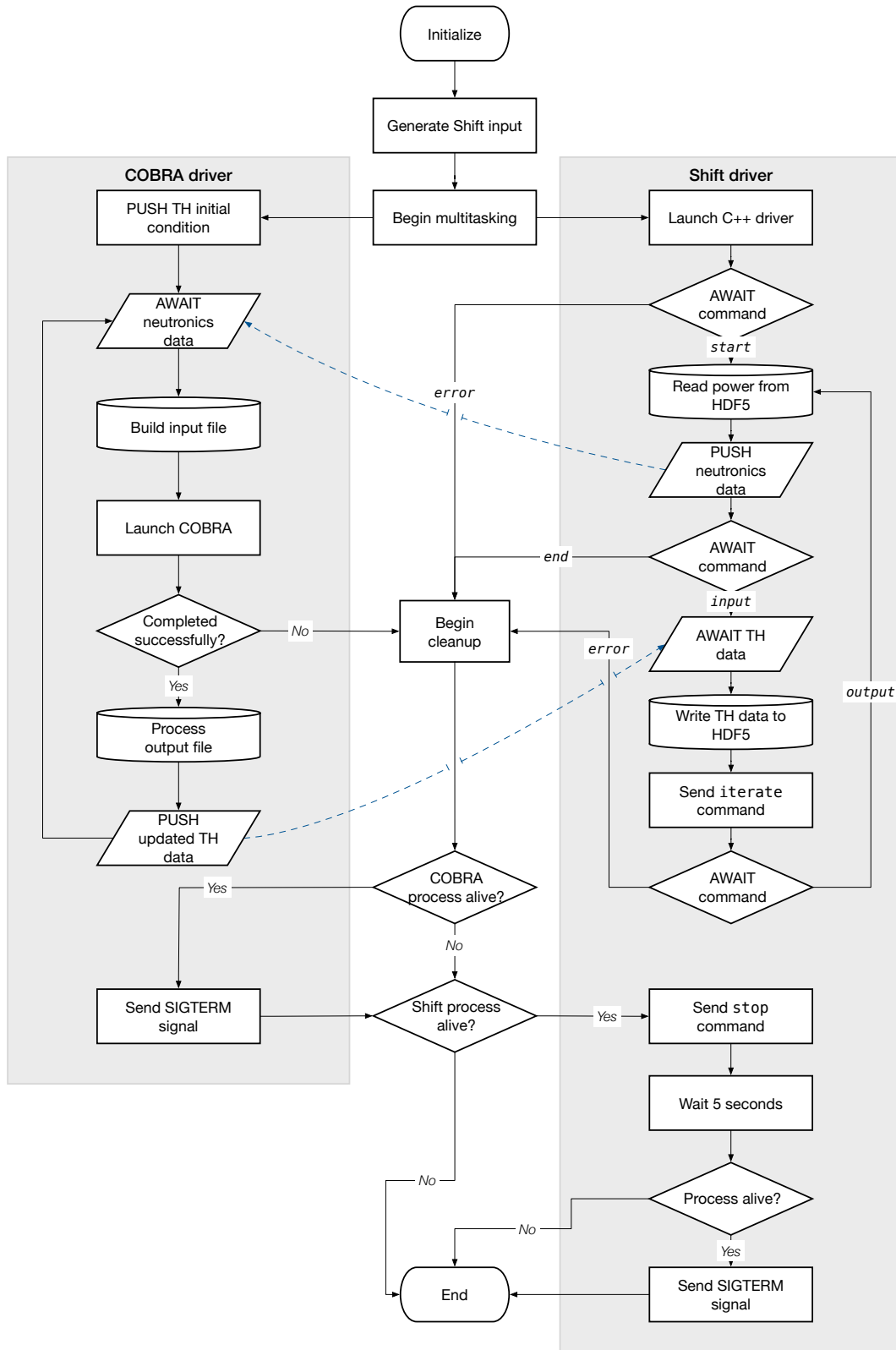


Figure 2. Multiphysics Coupling for a DPC Simulator for Solving Steady-State or Gradual Approach to Critical Configuration Problems.

2.2 Numerical codes

A brief description of the numerical codes used in the development of Terrenus is provided below.

2.2.1 Shift

Shift is a high-performance massively parallel Monte Carlo code featuring both continuous-energy and multigroup physics. Shift is capable of solving problems in both k-eigenvalue and fixed-source modes [5]. Shift can model coupled neutron/photon physics, including secondary particles born both by collisions and fission. Shift is also fully coupled to automatic cross section generation capabilities in the SCALE code package, as well as to ORIGEN for nuclide depletion and decay [6]. Shift has previously been used for SNF cask dose analysis [7].

Shift is highly optimized to work on high-performance computing platforms using multiple parallelization strategies that can be tailored to the memory and performance requirements of the target architecture. Internode parallelism is managed using an MPI-based communication paradigm in which the problem is decomposed into N_s sets with N_b blocks per set such that the total number of processes is $N_s \times N_b$. Particles are decomposed across sets, while the spatial domain is decomposed across blocks. Thus, setting $N_b = 1$ reverts to the traditional *domain replication* parallelism model in which only particles are decomposed, while $N_b > 1$ implies *domain decomposition*. For problems with large tally requirements, which are typical in many full model depletion problems, multiple blocks can be used to enable the problem to fit within memory limitations on each process.

In addition, Shift has recently [8] been enhanced with an intranode transport algorithm that uses NVIDIA graphics processing unit (GPU) hardware. Recent performance analyses show that as the number of nuclides in the model increases, on the latest NVIDIA compute GPU (Volta V100), Shift achieves a particle tracking rate equal to between 100–175 IBM Power9 compute cores. Furthermore, the efficiency is highest when large numbers of particle histories are simulated. Therefore, Shift is ideally suited to efficiently run the large particle count simulations necessary to reduce statistical convergence below the minimum uncertainty bounds required by this work.

The depletion package within Shift is also optimized to work on high-performance computing platforms. The depletion package does not attempt to maximize parallelism by simply evenly distributing the depletion regions among all available processes, since this would require the communication of the depletion results to be global. Rather, the depletion package exploits Shift's multilevel parallelism to reduce the amount of memory and communication required during solution of the depletion equations. A process only performs the depletion calculation on the depletable regions within its local block, with the depletion regions in a block evenly distributed across all sets. This maximizes the parallelism within a block while minimizing block-to-block communication. This depletion method has been shown to scale well to 10,000 cores [6]; however, since the depletion only constitutes a few percent (< 5) of the total simulation time, this performance is considered sufficient for the work proposed here.

As part of DOE's Advanced Scientific Computing Research (ASCR) Exascale Computing Project (ECP), Shift is being coupled to Nek5000, a spectral finite-element computational fluid dynamics (CFD) code [9] that can resolve turbulent flows using the large eddy simulation model. Capabilities developed during ECP will be leveraged for coupling to COBRA-SFS, including the use of on-the-fly doppler broadening of the cross sections, enabling tight coupling between the neutronics and thermodynamics.

Shift also has advanced hybrid deterministic / Monte Carlo capabilities for automatic variance reduction. This enables the rapid calculation of quantities of interest, even in low flux regions such as particle fluence on cask boundaries [10].

2.2.2 COBRA-SFS

COBRA-SFS is a program for steady-state and transient simulation of the thermal-hydraulic behavior of SNF systems [11, 12, and 13]. Like other codes in the COBRA family, such as COBRA-TF [14], COBRA-SFS solves a set of subchannel equations describing conservation of mass and momentum in the coolant flowing within fuel assemblies, as well as energy conservation within the fuel rods and other solid structures in the system. COBRA-SFS retains the validation history of other codes in the COBRA series, but it also provides additional validation specific to analysis of spent fuel systems. COBRA-SFS is distinguished from other COBRA variants by its treatment of features specific to spent fuel storage systems. This includes the ability to model natural circulation of coolant within a fuel cask, as well as simulation of radiative heat transfer between fuel rods and solid structures such as a spent fuel cask. It also extends the iteration scheme of other COBRA versions to be fully implicit in time to allow stronger coupling between equations governing fluid energy and heat transfer in solid components of the system.

2.3 Assumptions

Assumptions currently used in developing the Terrenus capability are discussed below. It is expected that some of these assumptions will be relaxed as the project moves forward.

- *Single-phase liquid:* It is assumed that boiling does not take place and that temperature and Doppler reactivity coefficients are sufficient to maintain criticality.
- *Drift space:* It is assumed that there is sufficient drift space between the canister surface and the repository wall to allow thermal convective and radiative processes.
- *Drift airflow:* It is assumed that airflow through the repository drift is essentially stagnant and that no ventilation exists during postclosure timeframe.
- *Water temperature:* It is assumed that water enters the DPC at the ambient temperature of the surrounding media.
- *Water flowrate:* It is assumed that inflow is equal to or greater than outflow, a condition necessary to maintain moderator presence within the DPC.
- *Configuration:* It is assumed that SNF is maintained at its original configuration.

2.4 Initial Configuration and Input Data

Shift supports a variety of geometric packages for modeling radiation transport scenes, including Monte Carlo N-Particle (MCNP) geometry, SCALE geometry, computer-aided design (CAD) geometry, and a reactor toolkit (RTK) geometry which was specifically designed for modeling PWRs for the Consortium for Advanced Simulation of Light Water Reactors (CASL) VERA code. The MCNP, SCALE, and CAD geometry packages enable modeling highly complex geometries, while the RTK package is limited to PWR geometries only.

However, there is much more to multiphysics simulations than simple geometric complexity. It is necessary to receive updated temperature and density information from the subchannel code and dynamically alter the model compositions. Because MCNP, SCALE, and CAD geometries are general purpose, they do not include the necessary model metadata denoting which geometric cells are fuel pins, which are guide tubes, which are moderator channels, etc. The only geometric package containing this metadata is the RTK geometry package. Therefore, it was decided that the more expedient and lower risk choice was to initially limit the Terrenus code to using RTK geometry models only. This enabled work to

focus on the multiphysics coupling aspects required by this milestone, deferring geometric complexity to a later time. This choice comes at the expense of limiting the models that can be simulated. This restriction will be eliminated in the future by creating a DPC-aware metadata layer on top of the general geometry (GG) package.

Several configurations (progression problems) have been developed and will be used to develop and demonstrate the progress of Terrenus multiphysics capabilities development. The selected configurations are listed below:

- a. A 3×3 square array of fuel rods with surrounding stainless steel walls on four sides, enclosed within a cylindrical stainless steel canister (used in this report)
- b. A 17×17 square array of fuel rods with surrounding stainless steel walls on four sides, enclosed within a cylindrical stainless steel canister
- c. A 3×3 square array of fuel assemblies enclosed within a cylindrical stainless steel canister, with each fuel assembly surrounded by a square stainless steel box that represents the canister basket
- d. A fully loaded canister with 37 PWR fuel assemblies, with each fuel assembly surrounded by a square stainless steel box that represents the canister basket
- e. A fully loaded canister with 37 PWR fuel assemblies, including a stainless steel basket and supporting structures
- f. A fully loaded canister with 89 BWR fuel assemblies, including a stainless steel basket, supporting structures, and an outer canister

Additional configurations may be used for benchmarking and validating various Terrenus modules.

Currently, Terrenus is capable of modeling any single PWR assembly within a cask, including fuel pins and guide tubes. However, for simplicity, the first progression problem (single 3×3 array of PWR fuel rods within a cask) was chosen as the test problem for this report. This problem is sufficient for demonstrating that the radiation transport and thermal-hydraulics modules are successfully coupled, but it does not require significant effort to set up; nor does it require significant computational resources: a perfect demonstration problem on an initial enabling capability. The details of the 3×3 pincell array are given below. For COBRA-SFS, the DPC cask walls were modeled explicitly, whereas with Shift, reflecting boundaries were set around the 3×3 array of pins. This was done to give the pincell array a higher reactivity, which is more similar to what would be experienced by a fully loaded cask. When cask-aware metadata have been added to the SCALE geometry package, multiple assemblies, as well as the DPC wall, will be modeled explicitly, the geometric scene will extend beyond the boundary of the DPC, and either vacuum boundaries or an albedo condition tuned to the repository's geology will be used.

Details of 3×3 square array of fuel rods

The configuration is shown schematically in Figure 3. Table 1 presents various fuel rod parameters as modeled in COBRA and Shift. Table 2 shows the fuel rod's material properties. Table 3 provides the square box and canister parameters. The backfill medium used is water at 14.7 psig pressure. Finally, Table 4 presents the backfill medium properties.

Table 1. Description of the Fuel Rod

Description	Values
Fuel rod outer diameter (in)	0.3740
Active fuel length (in)	144.0
Cladding thickness (in)	0.0243
Pitch (in)	0.4961
Pellet material	UO ₂
Cladding material	Zr-4
Enrichment (Weight %)	3% 235U

Table 2. Fuel Rod's Material Properties

Fuel cond.	Fuel Sp. heat	Fuel density	Pellet diameter	Clad. cond.	Clad. Sp. heat	Clad. density	Clad. Thickness
Btu/hr-ft-F	Btu/lbm-F	lbm/ft ³	in	Btu/hr-ft-F	Btu/lbm-F	lbm/ft ³	in
2.8	.0717	685.	.3669	9.540	.0779	409.	.0243

Table 3. Description of the Square Box and Canister

Description	Values
Square box thickness (in)	0.3937
Square box side length (in)	2.1104
Square box material	stainless steel
Canister inside diameter (in)	4.098
Canister thickness (in)	0.3937
Canister material	stainless steel

Table 4. Fluid Properties

Temp.	Enthalpy	Conduct.	Sp. heat	Sp. volume	Viscosity
°F	Btu/lbm	Btu/h-ft-°F	Btu/lbm-°F	ft ³ /lbm	lbm/ft-h
40	8.08	0.329	1	0.016	3.744
60	28.1	0.341	1	0.016	2.7108
80	48.1	0.352	1	0.0161	2.0736
120	88	0.371	1	0.0162	1.3464
160	128	0.384	1	0.0164	0.9612
180	148	0.388	1	0.0165	0.8352
200	168	0.391	1.01	0.0166	0.7308
212	180.16	0.3912	1.01	0.01671	0.6809

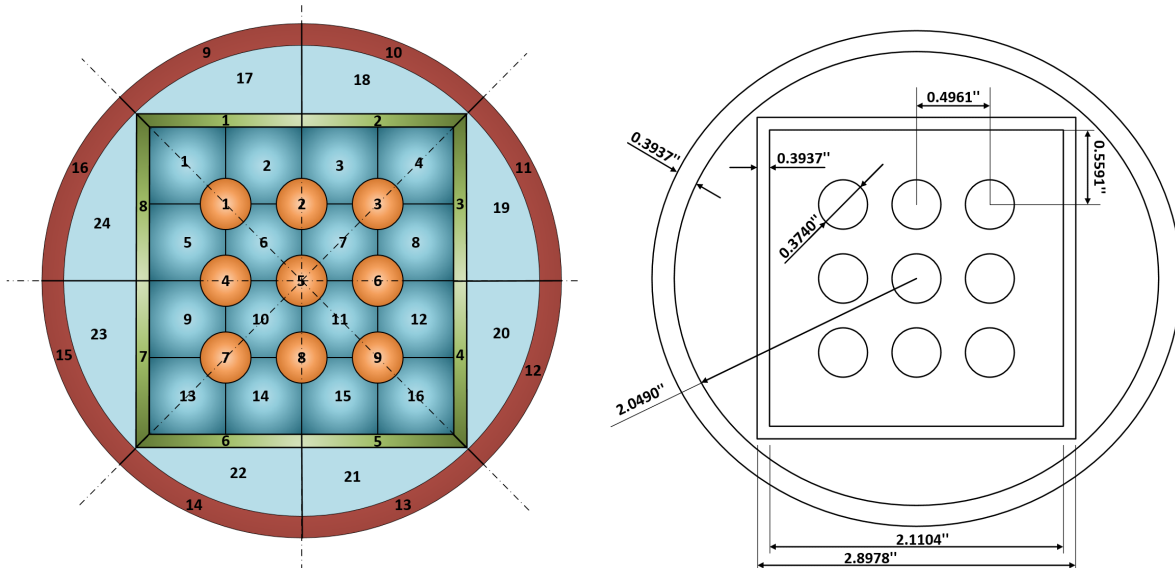


Figure 3. Schematic of 3×3 Square Array of Spent Fuel Rods within a Canister.
(The left image shows the COBRA-SFS channel, rod, and slab nodalization.)

3. RESULTS AND DISCUSSION

To demonstrate the new Terrenus code, a simplified, small DPC-style canister containing a 3×3 array of PWR fuel pins was simulated. The cask was modeled as 370.0 cm tall, and the fission heat was calculated at 12 evenly spaced axial levels along the cask height. A total power of 100 Watts was assumed. The outer boundary of the canister was assumed to be fixed at an ambient temperature of 60° F.

The radiation transport and thermal-hydraulics were allowed to run through 10 iterations. A convergence criterion of $1e-3$ was imposed on the fission power, which was calculated by the Shift code. However, it was found that the stochastic nature of the radiation transport solver caused non-monotonic statistical behavior in the fission power, such that the calculation appeared to never converge. (This is actually incorrect, as will be seen in the results described below.) This behavior indicates that more particle histories are required to be simulated to obtain a converged Monte Carlo solution. In addition, in the future, a convergence condition will be developed on the channel temperature and density fields. Since these are calculated from a deterministic subchannel computation, these fields are expected to be much more stable.

The powers were under-relaxed before being communicated to the subchannel code using

$$P^{i+1} = fP^{i+1,*} + (1 - f)P^i,$$

where P^{i+1} is the power at iteration $i+1$, $P^{i+1,*}$ is the just-calculated power from the radiation transport code, and f is the under-relaxation factor. Multiphysics simulations are nonlinear, and iterative coupling can often cause a given physics simulator to “over-shoot” the converged solution, thereby increasing the number of iterations necessary and reducing computational performance. There was insufficient time to perform a detailed analysis for optimizing the under-relaxation factor. For the simulation results given below, a factor of 0.7 was used. Future work will include a study to find the optimal under-relaxation parameter for various problems of interest.

The simulations were performed on a 2017 MacBook Pro using five MPI tasks. The 2017 MacBook Pro features 4 physical cores, but subchannel calculations were completed quickly enough for these small problems so that performance could be maximized by requesting 5 MPI tasks instead of only 4.

For each iteration, a Monte Carlo radiation transport simulation was performed with 25 inactive cycles, 25 active cycles, and 30,000 histories per cycle. This is perhaps not enough to obtain a converged solution, but sufficient for demonstrating the coupling capability. We do not currently reuse the converged fission source from the previous iteration, but this is a capability that we intend to add in the future that would reduce the number of inactive cycles necessary for all iterations after the first. Since the only concern was to demonstrate the coupling machinery, simplified compositions were used to reduce the computational expense of the radiation transport calculation. The fuel was low-enriched, fresh UO_2 containing only ^{16}O , ^{235}U , and ^{238}U . The gap was pure ^4He , and the clad was pure ^{90}Zr . The water was slightly borated to reduce the reactivity of the fresh fuel. Obviously, this is not realistic for SNF, but the reduced number of nuclides in fresh fuel significantly reduces the computational expense of the radiation transport without having any effect on the coupling performance under investigation here.

Fission power was calculated using a mesh tally placed over the pincell boundaries spanning 18 evenly spaced axial levels. The energy released per fission was calculated using the values in the ENDF-VII.1 libraries, which are 194.02 MeV/fission in ^{235}U and 198.122 MeV/fission in ^{238}U . Because COBRA-SFS does not support radiative heating in the channel, gamma heating was neglected. Future calculations could compute the gamma heating to gain more understanding of the consequence of this assumption.

3.1 Power Distribution

Figure 4 shows the radial power distribution for all 10 iterations at the midplane, $z = 185$ cm, of the 3×3 geometry. Physically, the power distribution should be perfectly flat. It can be seen that some iteration-to-

iteration statistical noise can be observed, although the variation is fairly modest (note the ranges of the color bars on the right of each image). Nevertheless, it may be necessary to run many more particles to obtain reduced variance and a more tightly converged fission source in future calculations.

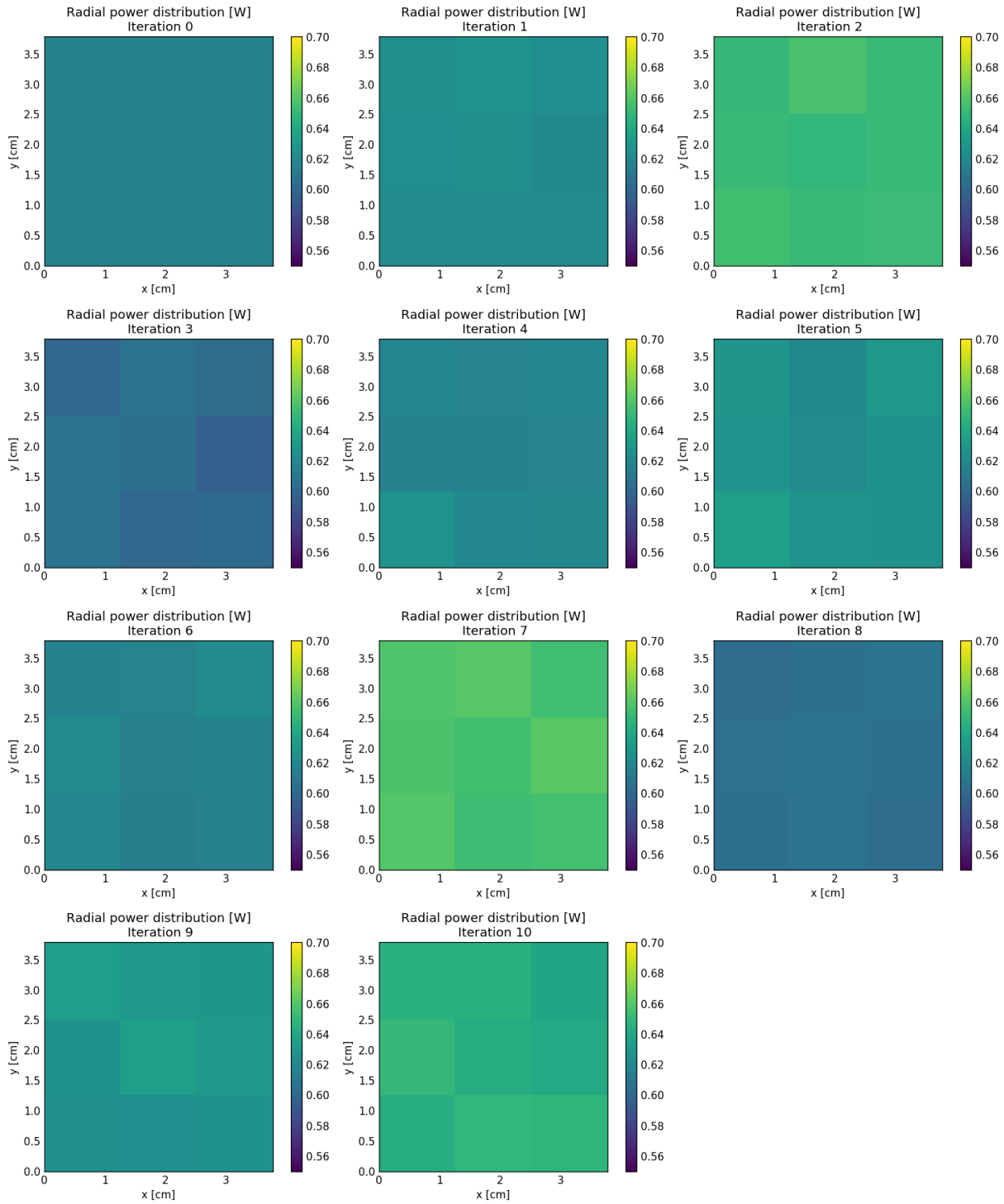


Figure 4. 3×3 Radial Power Distribution over 10 Iterations at $z = 185$ cm.

3.2 Channel Temperatures Distributions

Figure 5 shows channel temperatures for all 10 iterations. Iteration 0 starts with a uniform channel temperature at the ambient temperature of 60 °F. Subsequent iterations are obtained using the fission powers calculated by Shift. Here it can be seen that channel temperatures converge immediately with the first iteration, which suggests that the multiphysics simulation should be converged on channel properties rather than pin powers (as mentioned in Section 2) since these are more numerically stable. Convergence is rapid because the very low power of this critical assembly results in only a loose coupling between the neutronics and the thermal-hydraulics. A higher power would result in a tighter coupling requiring more iterations to converge. As expected, the inner channels are at a higher temperature because they are not adjacent to the cooler ambient temperature. It can also be observed that the channel in the top-left corner is slightly cooler than the other boundary channels. The cause of this is not clear since the model is symmetric in the x-y plane. One possibility is that statistical variations in the stochastic Monte Carlo radiation transport solution are causing a feedback loop between the transport and the thermal-hydraulics, thereby causing a nonphysical variation. Further investigation will be necessary to definitively answer this question.

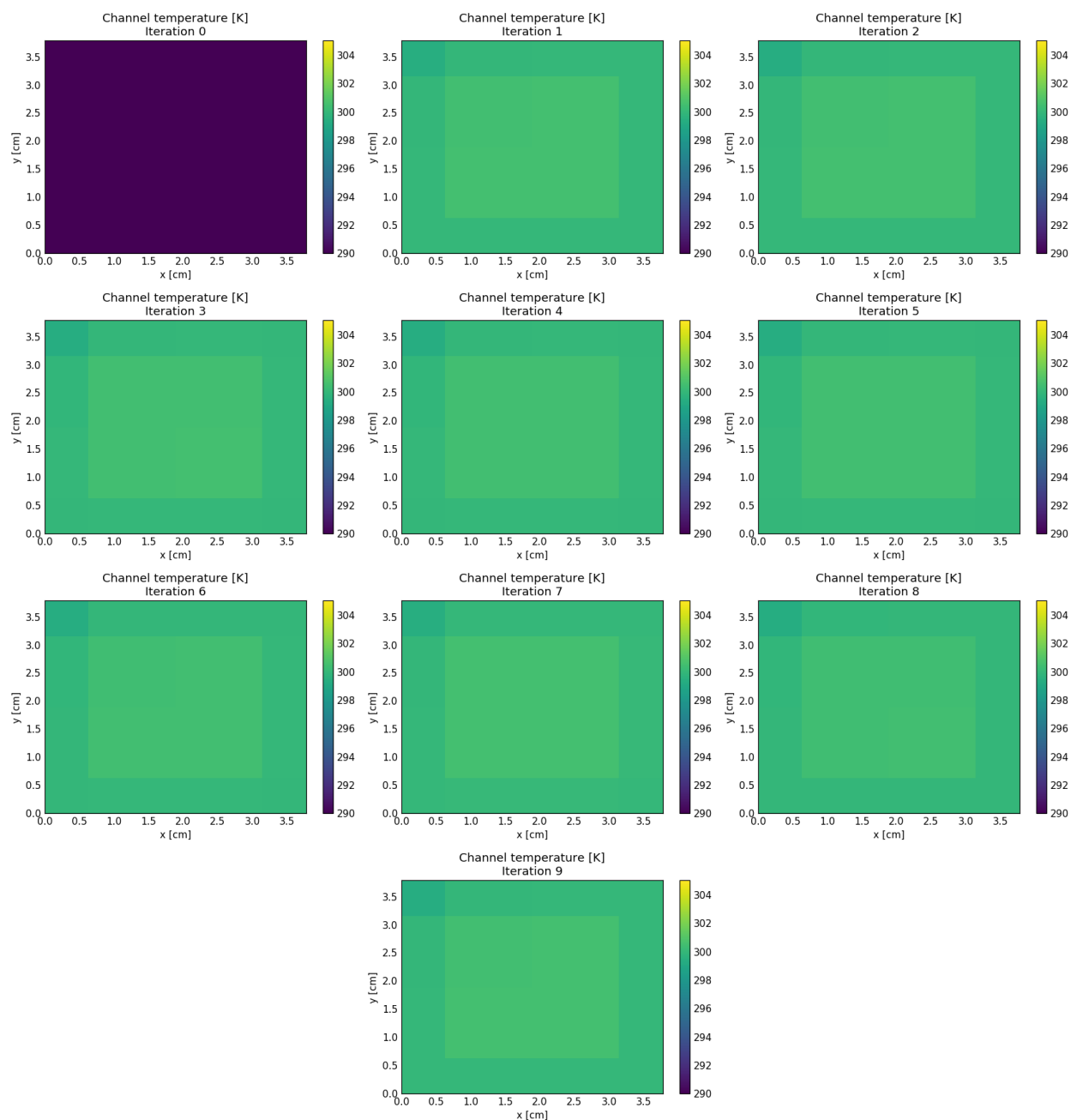


Figure 5. 4×4 Channel Temperatures over 10 Iterations at $z = 185$ cm.

Figure 6 shows the axial distribution of the temperature in one of the central channels. In this case, only iteration 0 and iteration 1 are shown since, as before with the radial distribution, the axial distribution converges immediately with the first iteration. The axial temperature distribution behaves as expected, with temperatures rising from the bottom to the top of the model.

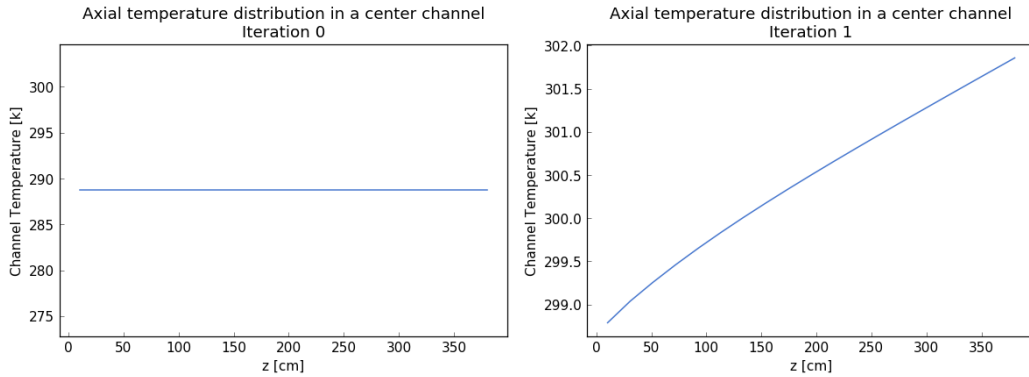


Figure 6. Axial Temperatures Distributions for Iterations 0 and 1.

3.3 Channel Density Distributions

Figure 7 shows the channel water densities. The initial condition is a channel water density of 1.0 g/cc. The channel densities converge in the first iteration. As expected, there is an inverse relationship between density and temperature, with lower densities in the center channels.

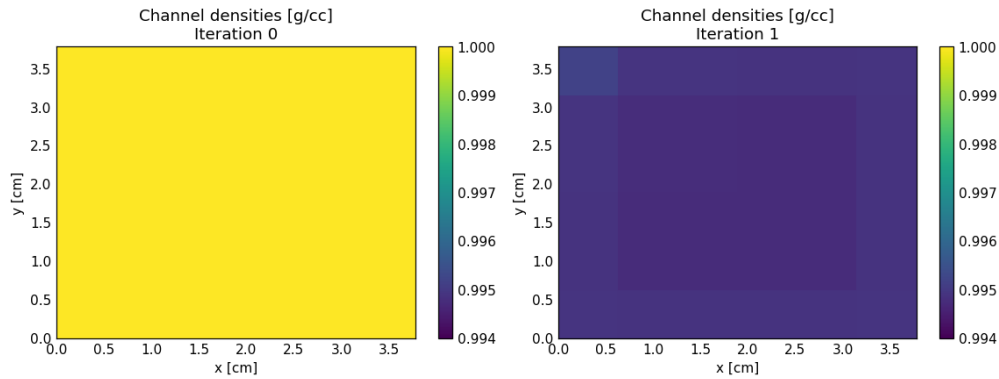


Figure 7. Channel Water Densities.

Figure 8 shows the axial water density distribution in a central channel. As expected, the density of the water is reduced as the temperature increases up the channel. As before, the axial density distribution is converged after the first iteration.

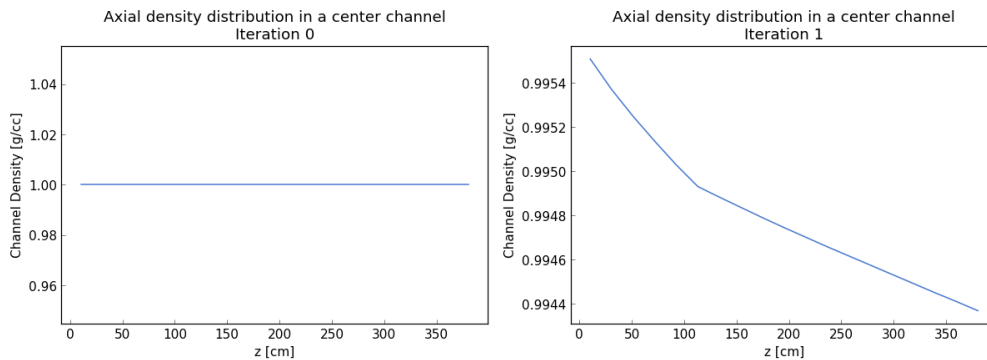


Figure 8. Axial Channel Water Densities in a Central Channel.

This page is intentionally left blank.

4. CONCLUSION

An initial multiphysics framework, Terrenus, has been developed to couple Monte Carlo radiation transport code Shift and thermal-hydraulics code COBRA-SFS. Currently, the Terrenus code is capable of coupling Shift and COBRA-SFS for a simplified cask model containing a single PWR assembly. The Terrenus framework has been tested using a simplified 3×3 fuel pin geometry.

Future work will expand the geometric capabilities of Terrenus so that a full cask of arbitrary reactor assemblies can be modeled, along with the cask internals. This will require adding an assembly-aware metadata layer onto the SCALE GG package within Shift, and it will also require a much more general-purpose COBRA input template.

Moreover, Terrenus currently requires the user to specify the total power of the system. Future work will include enabling Terrenus to calculate the negative temperature coefficient of the cask system so that a critical temperature search can be performed. The coupled transport thermohydraulics system will be able to iterate to the actual power. A new convergence criterion which uses the more stable thermal hydraulics parameters (channel temperature and density) rather than the stochastically noisy radiation transport parameter (power) will also be developed.

Finally, it is noted that it is far from clear that COBRA-SFS will be able to provide the thermal hydraulic functionality needed for this project over the long term. COBRA-SFS is a stand-alone code without any built-in coupling interface, which necessitated the complex Python coupling module that was developed. Because COBRA-SFS is single phase only, it cannot model boiling; nor can it calculate vapor pressure in a partially filled cask, which may be a major source of cask failure in criticality events. Finally, COBRA-SFS only runs on a single computational core. While the COBRA-SFS calculations were fast for the 3×3 demonstration problem presented in this milestone report, COBRA-SFS may become a serious performance bottleneck when scaling to full-sized cask models. Future work will include consideration of other thermal-hydraulic codes that may better meet the needs of the criticality consequence project.

This page is intentionally left blank.

5. REFERENCES

1. *StoreFuel and Decommissioning Report*, Ux Consulting Company, LLC (UxC), **21**, No. 248, (2019).
2. E. Hardin et al., *Investigation of Dual-Purpose Canister Direct Disposal Feasibility (FY14)*, FCRD-UFD-2014-000069 Rev.1, (2014).
3. J. B. Clarity, K. Banerjee, H. K. Liljenfeldt, and W. J. Marshall, “As-Loaded Criticality Margin Assessment of Dual-Purpose Canisters Using UNF-ST&DARDS,” *Nuclear Technology*, **199**(3), 245–275, (2017).
4. YMP (Yucca Mountain Site Characterization Project), *Disposal Criticality Analysis Methodology Topical Report*, YMP/TR-004Q, Rev. 02. Las Vegas, Nevada: Yucca Mountain Site Characterization Office, (2003). ACC: [DOC.20031110.0005](https://www.nrc.gov/docs/2003/1110.0005).
5. T. M. Pandya, S. R. Johnson, T. M. Evans, G. G. Davidson, S. P. Hamilton, and A. T. Godfrey, “Implementation, Capabilities, and Benchmarking of Shift, a Massively Parallel Monte Carlo Radiation Transport Code,” *Journal of Computational Physics* **308**, 239–272, (2016).
6. G. G. Davidson, T. M. Pandya, S. R. Johnson, T. M. Evans, A. E. Isotalo, C.A. Gentry, and W. A. Wieselquist, “Nuclide depletion capabilities in the Shift Monte Carlo code,” *Annals of Nuclear Energy* **114**, 259–276, (2018).
7. G. G. Davidson and K. Banerjee, *Initial Development of a Large Facility Dose Analysis Approach*. Prepared for DOE Spent Fuel Waste Disposition, SFWD-PO-2017-000084, ORNL/SPR-2017-/439, (2017).
8. S.P. Hamilton and T.M. Evans, "Continuous-energy Monte Carlo neutron transport on GPUs in the Shift code," *Annals of Nuclear Energy* **128**, 236—247, (2019).
9. E. Merzari, D. Pointer, and P. Fischer, “Numerical Simulation and Proper Orthogonal Decomposition of the Flow in a Counterflow T-Junction,” *Journal of Fluids Engineering*, **135**, (9), (2013).
10. J. C. Wagner, S. W. Mosher, T. M. Evans, D. E. Peplow, and J. A. Turner, “Hybrid and Parallel Domain-Decomposition Methods Development to Enable Monte Carlo for Reactor Analyses,” *Progress in Nuclear Science and Technology*, **2**, 815–820, (2011).
11. D. R. Rector, C. L. Wheeler, and N. J. Lombardo, *COBRA-SFS - A Thermal-Hydraulic Analysis Computer Code Volume I: Mathematical Models and Solution Method*, PNL-6049 Vol. I, (1986).
12. T. E. Michener, D. R. Rector, and J. M. Cuta, “COBRA-SFS Thermal-Hydraulic Analysis Code for Spent-Fuel Storage and Transportation Casks: Models and Methods,” *Nucl. Technol.*, **199** (3), 330–349, (2017).
13. T. E. Michener, D. R. Rector, and J. M. Cuta, “Validation of COBRA-SFS with Measured Temperature Data from Spent-Fuel Storage Casks,” *Nucl. Technol.*, **199**, (3), 350–368, (2017).
14. M. N. Avramova, *CTF: A Thermal Hydraulic Sub-Channel Code for LWR Transient Analyses*, User’s Manual, (2009).
15. A.T. Godfrey, “VERA Core Physics Benchmark Progression Problem Specifications, Rev. 4,” CASL-U-2012-0131-004 (2016).
16. K. BANERJEE et al., “Estimation of Inherent Safety Margins in Loaded Commercial Spent Nuclear Fuel Casks,” *Nucl. Technol.* **195**, 2 (2016).
17. RELAP5/MOD3 Code Manual, NUREG/CR-555, INEL-95/0174, Vol. 1: Code Structure, System Models and Solution Methods (1995).

This page is intentionally left blank.

Appendix A

This appendix documents work performed supporting the US Department of Energy (DOE) Nuclear Energy Spent Fuel and Waste Disposition, Spent Fuel and Waste Science and Technology, under work breakdown structure element 1.08.01.03.05, “Direct Disposal of Dual Purpose Canisters.” In particular, this appendix fulfills the M3 milestone, M3SF-19OR010305015, “Multiphysics criticality consequence analysis capability development status report,” as Revision 1 to M3SF-19OR010305016, “Initial neutronic and thermal hydraulic coupling for waste package” within work package SF-19OR01030501, “Direct Disposal of Dual Purpose Canisters–ORNL.”

In Section A.1, we expand on the results shown in Section 3 of this report by modeling a 17×17 pressurized water reactor (PWR) assembly and demonstrate multiphysics coupling between Shift and Cobra-SFS using Terrenus for this problem. In Section A.2, we demonstrate and discuss an initial investigation of various physical phenomena that can potentially decrease reactivity and quench a canister criticality event. In Section A.3, we show the results of an investigation of the water level necessary to achieve criticality in a typical SNF canister. In Section A.4, we describe the initial implementation of a critical power search capability. Finally, in Section A.5, we list conclusions and discuss future work.

A.1 Use of Terrenus on 17×17 PWR Assembly

To further test the performance of Terrenus, we performed a multiphysics analysis of a standard 17×17 PWR assembly. The model for this assembly was taken from Ref. [15]. The layout of a PWR assembly is given in Figure A.1. The pin diameters and material properties can be found in Ref. [15]. For our problems, we set the fuel enrichment at 2.0 wt % ^{235}U to maintain a moderate supercriticality. The water properties were the same as for the 3×3 pin array discussed in Section 2, and the boundaries of the problem were maintained at 60° Fahrenheit, just as with the 3×3 pin array.

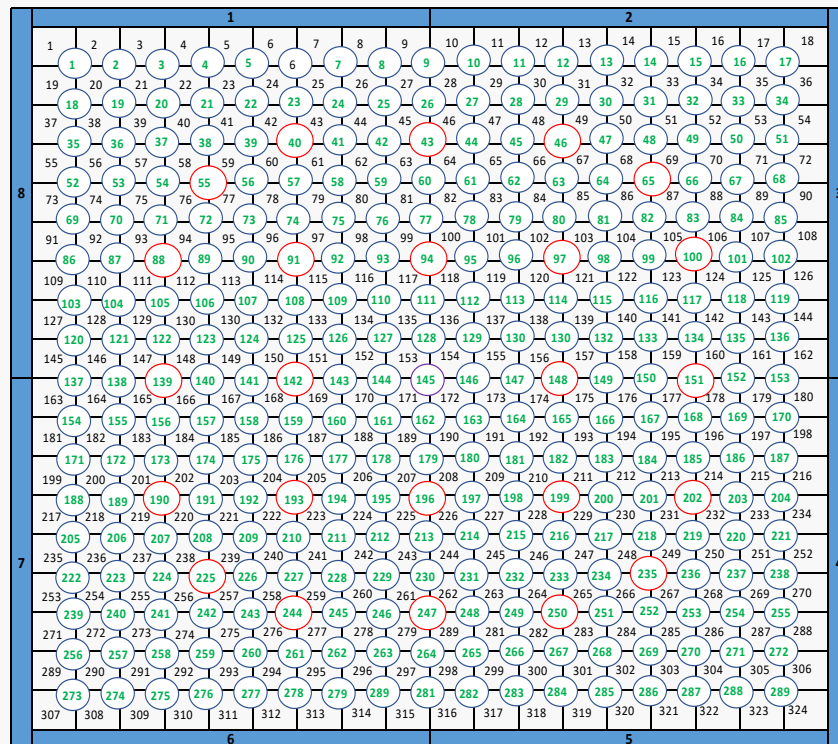


Figure A.1. Pin Layout of a Standard 17×17 PWR Assembly

In Figure A.2 (*left*) we show a plot of the relative pin powers at the axial midplane, and in Figure A.2 (*right*) we show a plot of the relative pin powers axially along one of the fuel pins adjacent to the central instrument tube. In both images, the powers behaved as expected. Power is zero in non-fuel pincells (i.e., in guide tubes and the instrument tubes) and has roughly a cosine shape axially.

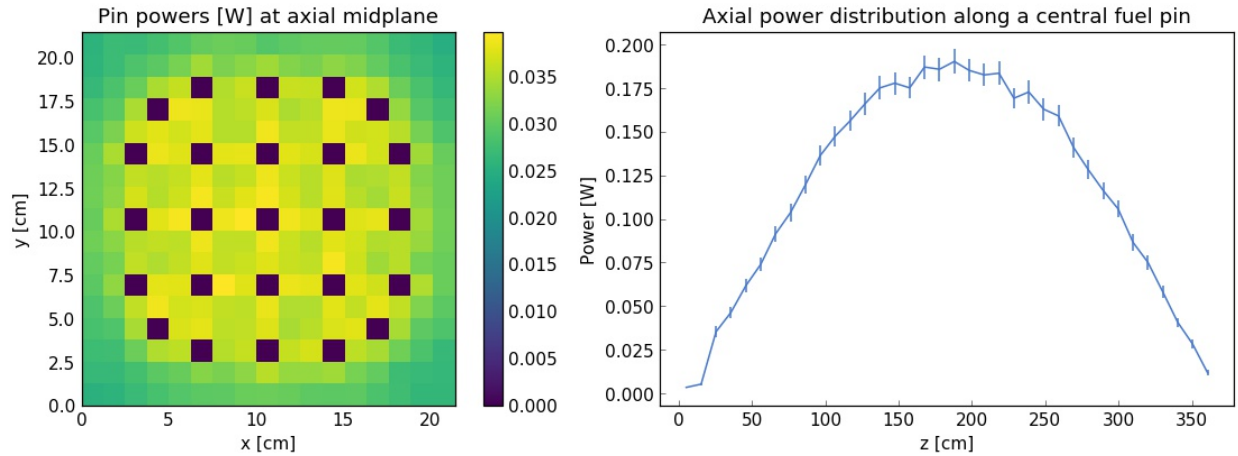


Figure A.2. Relative Pin Powers at the Axial Midplane (*Left*) and Axial Distribution of Relative Pin Power along a Fuel Pin adjacent to the Central Instrument Tube (*right*).

In Figure A.3 (*left*), we see the radial channel temperatures at the axial midplane, and Figure A.3 (*right*) shows the channel temperature axially through the central instrument tube. These results look as expected, with temperatures higher in the center of the PWR assembly and lower near the cooler boundary conditions. We also see the temperature rising monotonically axially through the assembly, as expected.

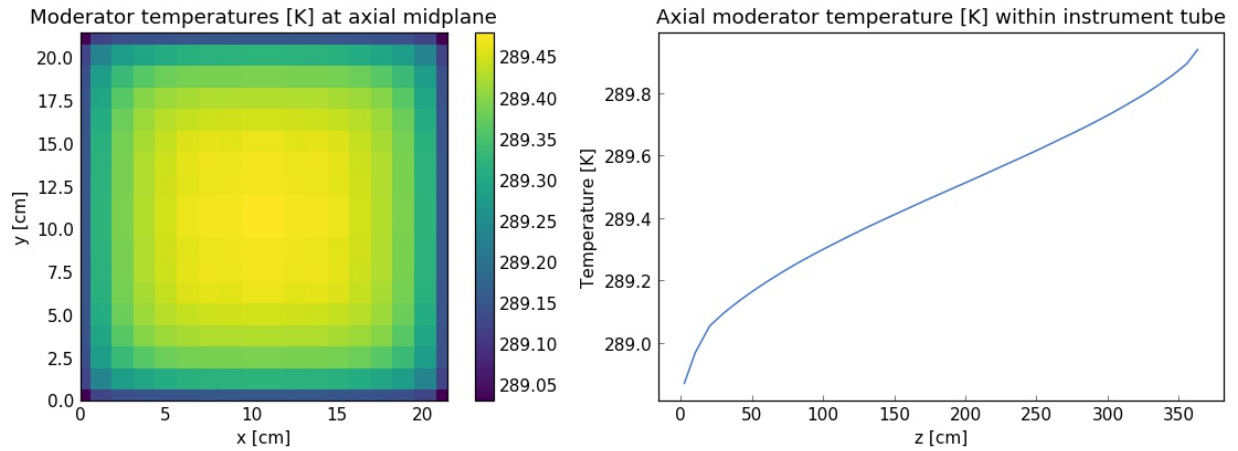


Figure A.3. Temperature of the Water Moderator in Each Channel at the Axial Midplane (*left*) and Axial Temperature Distribution in the Central Instrument Tube (*right*).

Figure A.4 (*left*) shows the radial water density in the channels at the axial midplane, and Figure A.4 (*right*) shows the axial water density in the central instrument tube. As expected, the density decreases with increased temperature, with higher density on the cooler boundaries of the PWR assembly and lower density in the warmer interior. The density also decreases monotonically axially through the assembly.

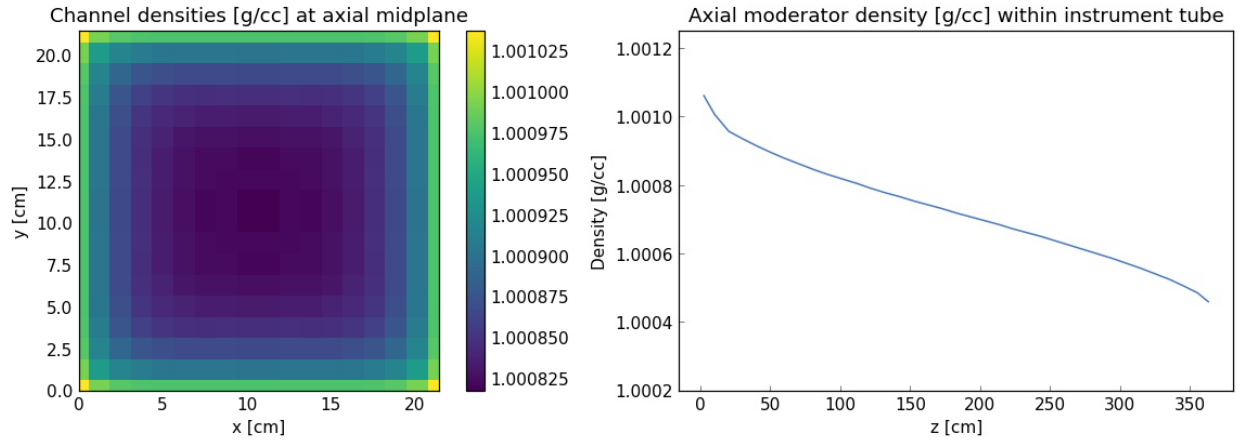


Figure A.4. Water Moderator Density in Each Channel at the Axial Midplane (*left*) and Axial Distribution of the Moderator Density in the Central Instrument Tube (*right*).

In Figure A.5 (*left*) we show the fuel pin temperatures radially at the axial midplane, and in Figure A.5 (*right*) we show the fuel pin temperature axially in a fuel pin adjacent to the central instrument tube. Again, the results are consistent with the channel temperatures and calculated powers and are consistent with the earlier 3×3 results presented in Section 3.

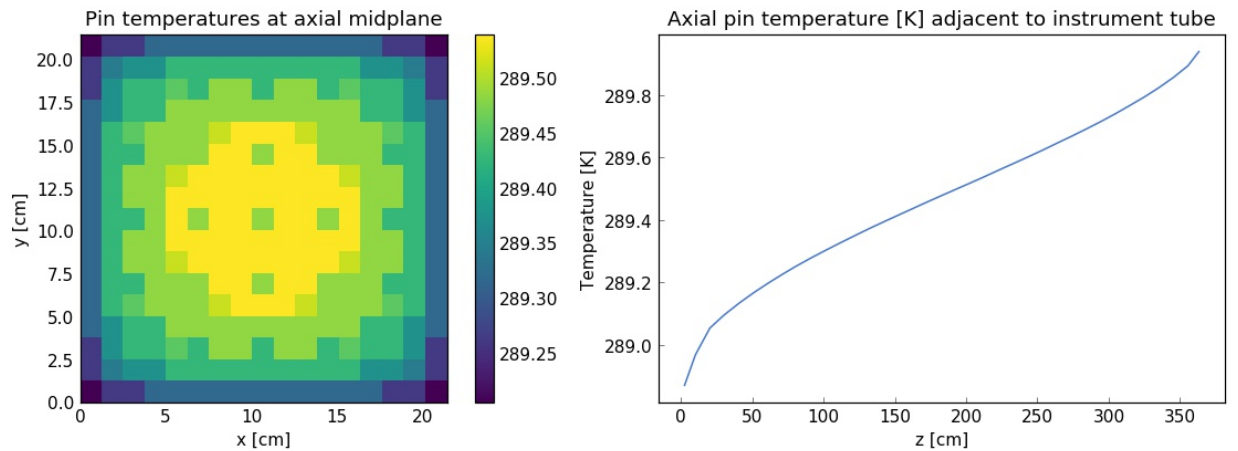


Figure A.5. Pin Temperature in Each Pincell at the Axial Midplane (*left*) and the Axial Temperature Distribution in a Fuel Pin adjacent to the Central Instrument Tube (*right*).

Finally, in Figure A.6 (*left*) and (*right*) we show the axial water temperature and water density in the central instrument tube for various power levels, respectively. For both plots, we observe what we expect: increased power generates increased water temperature and decreased water density.

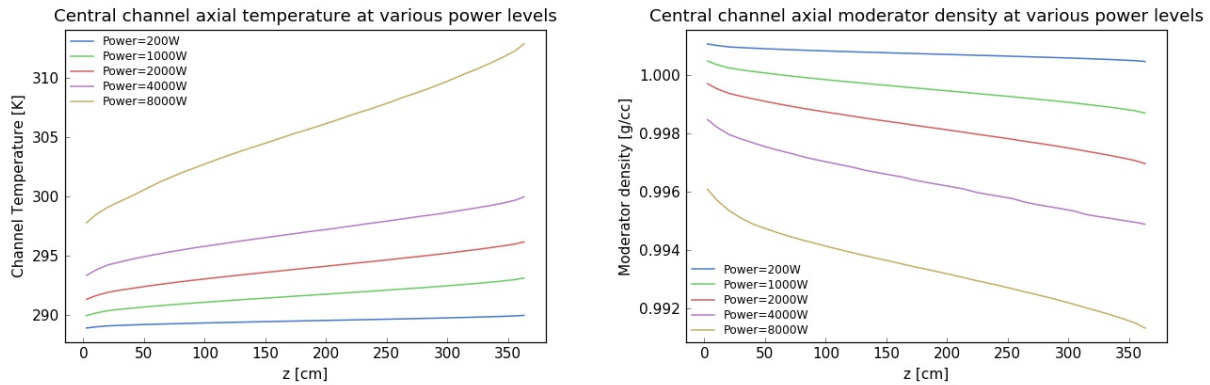


Figure A.6. Axial Distribution of Temperature (left) and Moderator Density (right) in the Central Instrument Tube for Various Power Levels.

A.2 Investigation of Negative Reactivity Phenomena

In this section, we discuss an initial investigation into the negative reactivity induced by various physical phenomena. First, we examine the negative reactivity caused by increased temperature. As the power level increases, the water temperature increases as well (as shown at left in Figure A.6). The water density also decreases; but since we are using reflecting neutronic boundaries, that effect is not captured. In Figure A.7, we show the effect of power level on reactivity for the 17×17 PWR problem. The modest increase in channel temperature has no effect on the criticality of the system. This corresponds to the typical experience in reactor physics, where negative temperature reactivity does not become significant until temperatures over 600 K are achieved.

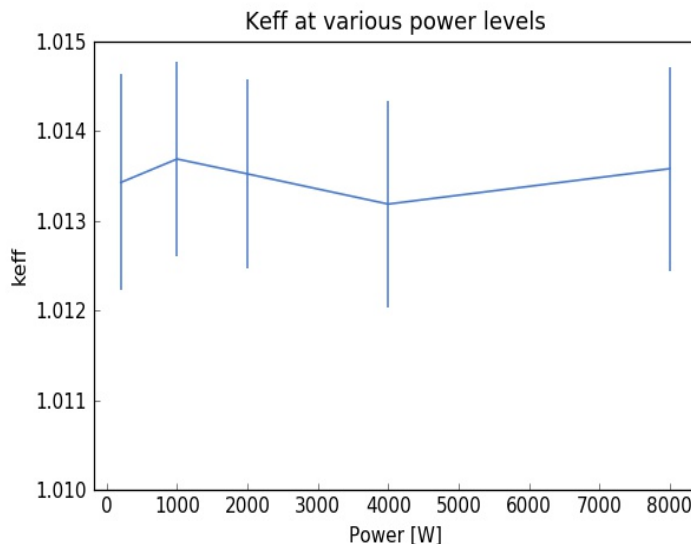


Figure A.7. Reactivity in a Fully Reflected 17×17 PWR Assembly at Various Power Levels.

Because the 17×17 assembly is surrounded by reflecting boundaries, decreases in moderator density have no effect, as a decrease in the mean free path through an infinite array of pins has very little effect. Therefore, to investigate the effect of changing moderator density on criticality, we created an array of assemblies similar to that of a loaded DPC, except that the canister walls were omitted and the assemblies

contained fresh fuel with a reduced enrichment of 1.0 wt % ^{235}U . The model geometry is shown in Figure A.8. The properties of each assembly are identical to those discussed in Section A.1, excepting the change to the fuel enrichment. A vacuum boundary was applied at all boundaries. Although Terrenus does not yet have the ability to perform multiphysics simulations of multiple assemblies, the underlying Shift Monte Carlo code can perform transport simulations of multiple assemblies.

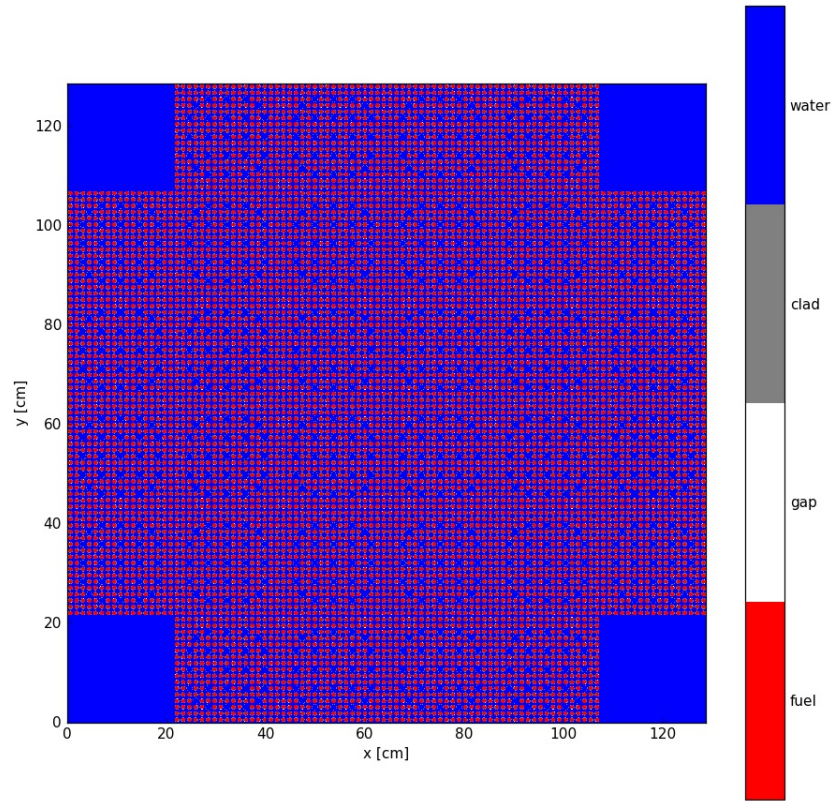


Figure A.8. A Simplified Neutronic Model of a Loaded Canister.

Therefore, we simulated the PWR model with Shift, varying the water density. The effect of varied water density on the reactivity is shown in Figure A.9.

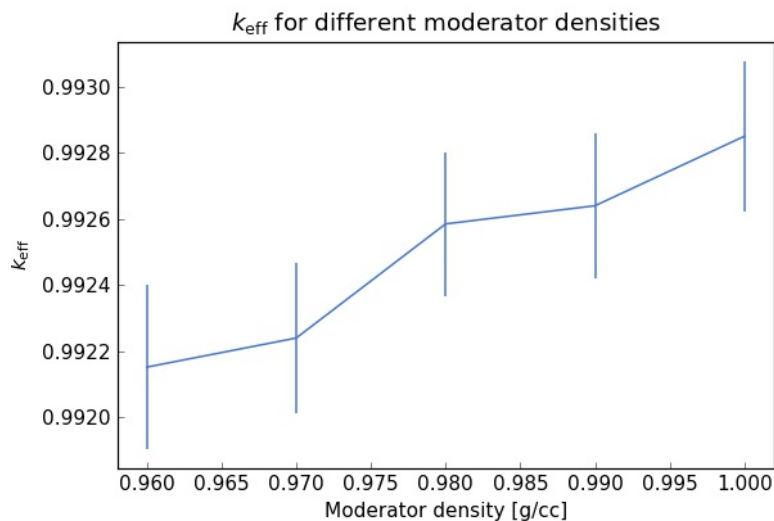


Figure A.9. Effect of Moderator Density on Reactivity.

We can see that as moderator density decreases, leakage from the system increases, and therefore k_{eff} decreases. We allowed the water density to span from 0.96 g/cc to 1.0 g/cc, which is approximately the range of densities that water can experience at 1 atm of pressure. We can see that while there was a clear trend in the value of k_{eff} , the differences were quite modest, spanning only 50 pcm.

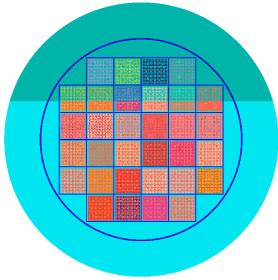
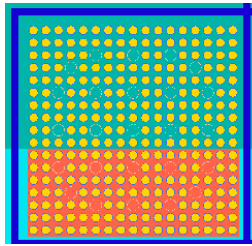
Although these results are still preliminary, we think it is unlikely that there is enough negative reactivity coefficient in a purely liquid water scenario to balance the excess reactivity of a critical canister. Therefore, it is likely that, in most situations, the water will boil; and it is the reduction in moderation due to the boiling that will keep the system from becoming supercritical.

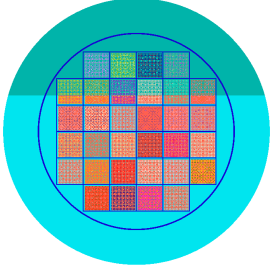
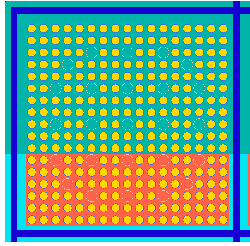
Our current thermohydraulic code, COBRA-SFS, is single-phase and does not support boiling. Our plans for addressing this shortcoming are addressed in Section A.4.

A.3 Calculating Critical Water Level

To gain insight into critical configurations for typical SNF canisters, a series of criticality calculations were performed using Shift to determine the critical water level for a realistic MPC-32-TSC canister. The radiation transport models were generated with UNF-ST&DARDS [16], which uses operational data to build as-loaded casks with used fuel assemblies. All of the casks generated with the UNF-ST&DARDS tool were completely submerged in water and had to be modified to simulate a canister that was only partially filled. We note that this was a non-trivial task that required substantial analyst effort. Our intention is that in the future, Terrenus will be able to create the necessary models automatically for calculating a critical water level. Once the models were generated, a simple criticality search was conducted to narrow down the precise water level that yielded a multiplication factor nearest to unity. The final result is illustrated in Table A.1, which shows the two bounding cases that narrowed down the critical water level for the Sequoyah MPC-32-TSC 079 canister. Note that a similar analysis could be performed for any potentially critical canister. For this particular canister, the critical water level was approximately 103 cm from the bottom of the first row of assemblies.

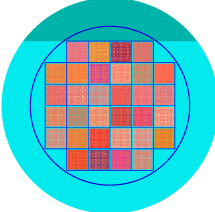
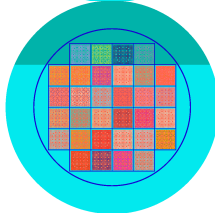
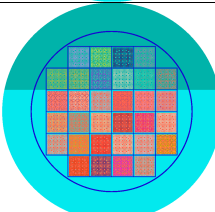
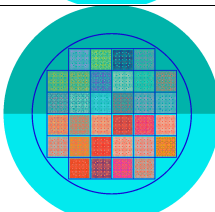
Table A.1. Critical Water Level for the MPC-32-TSC 079 Sequoyah Canister

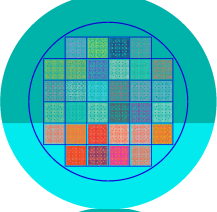
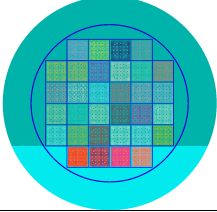
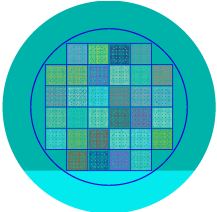
Cask Cross-section	Water Level	Assembly Cross-section	Multiplication Factor (k_{eff})
	~103.61 cm		1.00016506 ± 6

	<p>~102.37 cm</p>		<p>0.9994745 ± 5</p>
---	-------------------	--	----------------------

Before deciding upon the Sequoyah MPC-32-TSC 079 canister, a couple of other cases were run, including a cask with fresh fuel and another that did not achieve criticality even when completely submerged. The results from these cases are shown in Table A.2 alongside the Sequoyah 079 case. Note that the majority of the canisters considered in this investigation did not have a multiplication factor above unity, even when completely flooded. Of the ~ 27 canisters available in the UNF database from the Sequoyah facility, only 4 went critical when completely submerged in water. All of the cases investigated were decayed for approximately 20,000 years and included no neutron absorbers.

Table A.2. Test Cases for Critical Water Level Search

Cask Cross-section	Water Level	Multiplication Factor (k_{eff})		
		Fresh Fuel	Used Fuel	Sequoyah 079
	<p>~ 141 cm</p>	<p>1.10353</p>	<p>0.99773</p>	<p>1.00957</p>
	<p>~ 117.5 cm</p>	<p>1.10023</p>	<p>0.99629</p>	<p>1.00743</p>
	<p>~ 94 cm</p>	<p>1.09115</p>	<p>0.98744</p>	<p>0.99824</p>
	<p>~ 70.5 cm</p>	<p>1.07437</p>	<p>0.96796</p>	<p>0.97979</p>

	~ 47 cm	1.03492	0.93414	0.93941
	~ 23.5 cm	0.93026	0.84492	0.84941
	~ 0 cm	0.33254	0.27118	0.27183

A.4 Initial Implementation of Critical Power Search

Ultimately, we wish to use Terrenus to calculate the power produced by a fully loaded, fully or partially flooded SNF canister. The power produced by a critical canister is determined by a balance between the thermohydraulic and heat-transfer properties of the system and the neutronics. A canister with excess criticality (k_{eff} above 1.0) will cause an increase in moderator and fuel pin temperature and a decrease in moderator density. As was discussed previously, these phenomena are insufficient to reduce k_{eff} by a significant amount. However, once the water begins to boil, the increased void fraction will cause a substantial reduction in the population of thermal neutrons, thereby bringing the reaction into balance.

To calculate this critical power, we began with an initial guess of what the power level might be, as well as an initial guess of the negative power reactivity coefficient (i.e., the negative change in the reactivity for every increased watt of power). It is required by the physics of the system that the reactivity decrease as the power increases. Using the initial guess of the power, the thermohydraulic properties and the reactivity are computed by COBRA-SFS and Shift, respectively. Using the reactivity calculated by Shift, a new power level and new negative reactivity coefficient are calculated. These are then iterated to convergence.

This capability has been implemented into Terrenus but cannot be tested until boiling can be modeled. As discussed in Section A.5, this modeling can be done approximately in COBRA-SFS or more exactly with an alternative code such as Relap-5 [17].

A.5 Conclusions and Future Work

We have expanded the capabilities in Terrenus from a 3×3 array of pins to a full 17×17 PWR assembly. We note that we are still using a simplified fresh fuel definition instead of spent fuel. We confirmed that the multiphysics simulations produce results consistent with expectations: that water temperature rises

and density falls axially as water flows up the fuel channels. We also confirmed that the power profile and pin temperatures look as expected, with a uniform power profile radially in the fuel pins, no power in the guide and instrument tubes, and a roughly cosine shape in the axial direction.

We also investigated what physical phenomena are likely to balance excess reactivity in a flooded canister. We found that neither increased fuel temperature nor decreased water density is likely to be sufficient to balance even small amounts of excess reactivity. Therefore, it is likely that the water temperature will increase until boiling occurs. It will be necessary to model boiling in the future.

Finally, we investigated the critical water level for a typical SNF canister. The model necessary for this analysis was produced by hand, but in the future we intend for Terrenus to produce these models automatically.

Our near-term plans for Terrenus include the introduction of boiling physics for the thermohydraulic solver. There are two ways to do this. The first is to attempt to approximate boiling using COBRA-SFS with a homogeneous equilibrium model. This approximation will likely calculate the conduction of heat away from the fuel pins nearly correctly but will introduce error into the calculation of heat convection. Whether this error would be acceptably small is unknown. An alternative is to replace COBRA-SFS with a thermohydraulic code that has a boiling model. One possibility is to use RELAP-5 or RELAP-7 for this purpose. We are investigating this alternative.

We intend to continue to expand the neutronic modeling capabilities of Terrenus as well by enabling the simulation of multiple assemblies as well as the canister walls and interior neutron absorber panels. Additionally, Terrenus currently requires four input files: a Terrenus input file, a Shift input file, a model geometry file, and a COBRA-SFS file. Ensuring that all of these input files are correct and consistent with one another is time consuming and error prone. In the future, we intend to use a single Terrenus input file and have Terrenus automatically generate any other input files that are required.

This page is intentionally left blank.